J|A|C|S
COMMUNICATIONS

Published on Web 03/02/2006

CEESY: Characterizing the Conformation of Unobservable Protein States

Hugo van Ingen, Geerten W. Vuister, Sybren Wijmenga, and Marco Tessari*

Department of Physical Chemistry, Radboud University Nijmegen, Toernooiveld 1, 6525 ED, Nijmegen, The Netherlands

Received October 7, 2005; E-mail: tessari@nmr.ru.nl

Many biological processes such as ligand binding, enzyme catalysis, allosterics, and protein folding involve conformational rearrangements on a micro- to millisecond time scale to transient protein states with a low population, also termed excited states.[1] These unobservable minor states can only be studied indirectly by exploiting their continuous interconversion into the major or ground state. Kinetic and thermodynamic parameters of this exchange process can be determined along with the frequency difference between excited and ground state for a number of backbone and side-chain nuclei using well-established relaxation dispersion techniques.[2] These frequency differences are of great interest because they allow the structural characterization of the excited-state, provided their sign is known.[3] However, only the absolute value is accessible using relaxation dispersion methods. Experiments to measure the sign have so far only been designed for backbone ^{15}N nuclei.[4,5] Here, we present a new method, named CEESY (for Chemical Exchange to Excited States spectroscopY), to establish the sign of the frequency difference between ground- and excited-state signals using a single 2D spectrum. Importantly, this method is not limited to ^{15}N but can also be applied to most relevant spins in bioorganic materials and will, therefore, allow for a more complete spectroscopic characterization of the excited state.

The essential pulse sequence element of the CEESY (Pronounce as /'keisi:/ (International Phonetic Alphabet notation)) experiment involves two heteronuclear spins *I* and *S* (Figure 1a). It consists of a modified spin-echo sequence comprised of two periods of duration τ, separated by a refocusing 180° pulse on spin *S*. Single quantum *S* spin coherence evolves in the first τ period and *IS* multiple quantum coherence in the second τ period. In the absence of exchange, the chemical shift evolution of spin *S* is completely refocused and a perfect echo is obtained at point *a*. Conversely, chemical shift refocusing is only partially achieved in the presence of exchange, as a result of a difference in the exchange induced shift for SQ and MQ coherences[4] and a small net rotation of *S* coherence at point *a* results (Figure 1b,c). Thus, a large, *main* component (projection on echo axis) and a small, *orthogonal* component (projection on orthogonal axis) are present at the end of this modified spin-echo. The sign of this rotation is determined by the sign of the Larmor frequency difference between excited and ground-state resonances in most cases of practical interest, i.e., fast-to-intermediate two-site exchange.[4] Observation of identical signs for the two components can therefore be directly translated into an increased Larmor frequency in the excited state ($\omega_{S,e} > \omega_{S,g}$), while opposite signs denote a decreased Larmor frequency in the excited state with respect to the ground state ($\omega_{S,e} < \omega_{S,g}$). The signs of the two components can readily be obtained by a proper choice of the phase ϕ of the 90° pulse on spin *S* at time point *a* (Figure 1a). The CEESY building block is robust with respect to interferences from *J*-couplings and cross-correlated relaxation. The requirement for two-site exchange is not so restrictive. In the case of multisite exchange, meaningful average spectral information on the conformations in the ensemble of excited states can be obtained.[2a]

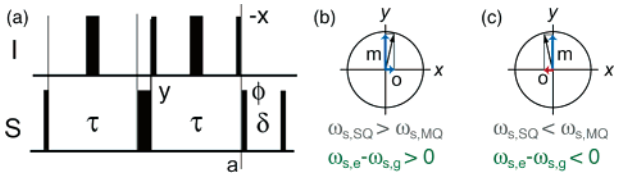

Figure 1. (a) Diagram of the CEESY pulse sequence element. Narrow (wide) bars represent 90° (180°) pulses along the *x*-axis unless indicated otherwise. (b,c) In the presence of exchange to an excited state, the echo formed at time point *a* is rotated. The relative sign of the orthogonal (o) and main (m) component matches the sign of the frequency separation between excited and ground state. Passive heteronuclear *J*-couplings involving either spin *I* or *S* are refocused. Passive homonuclear couplings introduce a scaling factor $\cos(\pi J_{S-S}2\tau)$ that identically affect the orthogonal and main component. Double antiphase terms $4I_zS_xS_z$ and $4I_zS_xS_y$, generated by homonuclear coupling J_{S-S}, are removed by the *z*-filter. Cross-correlation effects are suppressed by the 180° pulses on spin *I*.

We have applied the approach outlined above to determine the sign of the frequency difference for the amide proton ^{1}H$_N$ ($\Delta\omega_{HN} = \omega_{HN,e} - \omega_{HN,g}$) and the backbone ^{15}N nuclei ($\Delta\omega_N = \omega_{N,e} - \omega_{N,g}$). CEESY experiments for ^{1}H$_N$ and ^{15}N were tested on the 12 kDa PAH2 protein domain, for which fast-to-intermediate conformational exchange has been observed between a structured form and a low-populated, partially unfolded state.[6] The CEESY building block was inserted in a regular sensitivity enhanced HSQC (pulse sequences and experimental parameters shown in Supporting Information) and for both the main and the orthogonal component a 2D ^{15}N,^{1}H correlation spectrum was recorded.

Positive and negative peaks were found in the 2D spectrum of the orthogonal component for both ^{1}H$_N$ and ^{15}N nuclear spins. Representative results are shown in Figure 2. Starting with the ^{1}H$_N$ CEESY, panel (a) shows the main component of the echo for residue L22 in three spectra recorded with increasing duration of the spin-echo delay τ. These 1D traces demonstrate the decay of signal intensity due to relaxation and exchange. In panel (b) the traces for orthogonal components of residues L22, D23 and Q98 are plotted. For L22 a negative signal is observed, whose magnitude increases with increasing spin-echo delay. Likewise, an increasing positive signal is seen for D23. For Q98, no signal is observed, implying negligible chemical exchange for the ^{1}H$_N$ nucleus of this residue. Panel (c) displays two typical results of the ^{15}N CEESY. A clear, negative signal is observed for L22, and a positive peak for D23.

As discussed above, opposite signs for the two components imply a smaller Larmor frequency in the excited state with respect to the ground state, while identical signs indicate a larger Larmor frequency in the excited state. To translate this into a chemical shift difference, one has to consider that the direction of the frequency axis runs in opposite directions for ^{1}H and ^{15}N as it depends on the sign of the gyromagnetic ratio.[7] Thus, the ^{1}H$_N$ and

10.1021/ja0568749 CCC: $33.50

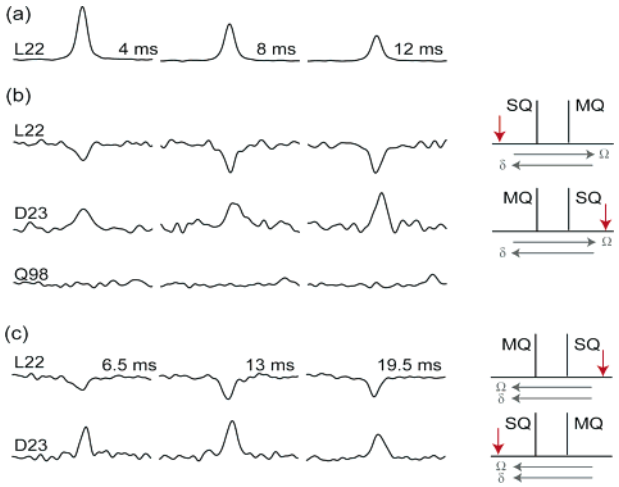

Figure 2. Representative results of the $^{1}H_N$ (a,b) and ^{15}N CEESY (c), showing slices through the peak maximum along the acquisition axis of the 2D spectrum. (a) main component of L22 at three echo delay values (indicated above the traces). (b) Orthogonal component of L22 (decreased $\omega_{HN,e}$), D23 (increased $\omega_{HN,e}$) and Q98 (no exchange). (c) Orthogonal components of L22 (decreased $\omega_{N,e}$) and D23 (increased $\omega_{N,e}$). Stick spectra on the right indicate the corresponding relative positions of ground state SQ- and MQ-peaks and the excited-state resonance (red arrow). Directions of the frequency and chemical shift axis are shown with gray arrows. Data acquired on 0.9 mM uniformly $^{13}C/^{15}N$ labeled PAH2 sample at 11.7 T, 298 K and a room-temperature probe head.

^{15}N resonances of L22 (δ_{HN} 7.3 ppm; δ_N 126.0 ppm) are shifted to higher and, respectively, lower ppm values in the excited state. The opposite behavior was found for D23 (δ_{HN} 8.7 ppm; δ_N 113.1 ppm), with $^{1}H_N$ and ^{15}N resonances shifted to respectively lower and higher ppm values in the excited state. For both residues these results indicate a resonance shift toward the random coil values, consistent with a less structured excited state.[6]

The sign of $\Delta\omega_{HN}$ and $\Delta\omega_N$ was classified using the 2D spectrum of the orthogonal component recorded with the longest spin-echo delay (i.e., τ is 12 ms for $^{1}H_N$ and 19.5 ms for ^{15}N). Taking a conservative approach, only those signals were considered for which the spin-echo was rotated by more than 1° and for which the intensity, $|I_{ortho}|$, exceeded 3 times the noise level. The maximum rotation observed, defined as $\arctan(I_{ortho}/I_{main})$, was $-5 \pm 1°$ for the $^{1}H_N$ CEESY and $+19 \pm 2°$ for the ^{15}N CEESY. Out of 72 nonoverlapping resonances, 15 $\Delta\omega_{HN}$ and 34 $\Delta\omega_N$ signs could be classified. The latter accounts for nearly all residues with significant dispersion of their ^{15}N transverse relaxation rates (Figure 3). Notably, even for the fast-relaxing amide proton a significant number of $\Delta\omega$ signs were determined. Interestingly, $\Delta\omega_N$ and $\Delta\omega_{HN}$ have opposite signs for 10 out of 13 possible comparisons.

To validate the CEESY method, the sign of $\Delta\omega_N$ was also determined using the H(S/M)QC approach, as proposed by Skrynnikov et al.[4] A triplicate set of interleaved HSQC and HMQC spectra was recorded and using a threshold of 0.3 Hz,[4] 16 signs could be classified, which were found in perfect agreement with the outcome of the ^{15}N CEESY experiment (Figure 3). Only 9 out of these 16 residues showed differences in ^{15}N peak position beyond 1 Hz, with a maximum of 3.2 Hz and an average of 1.1 Hz (taking absolute values). These small differences in peak position are related to the low population (ca. 1%) of the excited state.[6] Since the sensitivity of the CEESY experiment is primarily limited by signal-to-noise and spectral analysis is less hampered by signal overlap, a more complete classification of the sign of the shift difference $\Delta\omega$ was possible, even in this case of extremely skewed populations.

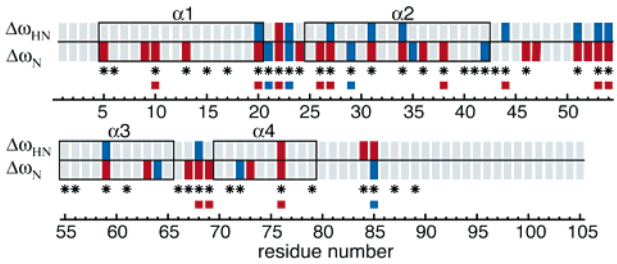

Figure 3. Resulting signs (red: negative; blue: positive) of $\Delta\omega_{HN}$ (top row) and $\Delta\omega_N$ (bottom row) between ground and excited state. Boxes indicate helices. Stars indicate residues with significant dispersion of $^{15}N-R_2$ rates.[6] Signs of $\Delta\omega_N$ from the H(S/M)QC method are shown with squares.

In conclusion, we propose a new method to determine the position of unobservable excited-state resonances relative to the observed resonances using a single 2D spectrum. The obtained information is crucial for the structural characterization of excited states. Our CEESY experiment can be applied to proteins, nucleic acids, or any system in fast-to-intermediate two-site exchange. Here, we have reported the experimental determination of the sign of $\Delta\omega$ of the backbone nitrogen and, for the first time, of the amide proton. Importantly, this approach can be extended to different nuclear species. We anticipate that application to other nuclei, such as the C_α and C_β of proteins, will provide spectroscopic information to characterize the structure of unobservable protein conformations in more detail. Ultimately, combination of relaxation−dispersion and CEESY experiments applied to multiple backbone nuclei will allow main-chain structure determination of these excited states.

Acknowledgment. We thank Prof. Dr. Cees W. Hilbers for his interest, and NWO for financial support (Grant JC 99-03).

Supporting Information Available: Pulse sequences (Varian pulse sequence available upon request) and detailed results. This material is available free of charge via the Internet at http://pubs.acs.org.

References

(1) (a) Mulder, F. A.; Mittermaier, A.; Hon, B.; Dahlquist, F. W.; Kay, L. E. *Nat. Struct. Biol.* **2001**, *8*, 932−935. (b) Volkman, B. F.; Lipson, D.; Wemmer, D. E.; Kern, D. *Science* **2001**, *291*, 2429−2433. (c) Eisenmesser, E. Z.; Bosco, D. A.; Akke, M.; Kern, D. *Science* **2002**, *295*, 1520−1523. (d) Korzhnev, D. M.; Salvatella, X.; Vendruscolo, M.; Di Nardo, A. A.; Davidson, A. R.; Dobson, C. M.; Kay, L. E. *Nature*, **2004**, *430*, 586−590. (e) Dyson, H. J.; Wright, P. E. *Methods Enzymol.* **2005**, *394*, 299−321.

(2) (a) Palmer, A. G.; Kroenke, C. D.; Loria, J. P. *Methods Enzymol.* **2001**, *339*, 204−238. (b) Akke, M. *Curr. Opin. Struct. Biol.* **2002**, *12*, 642−647. (c) Palmer, A. G.; Grey, M. J.; Wang, C. *Methods Enzymol.* **2005**, *394*, 430−465. (d) Ishima, R.; Torchia, D. A. *J. Biomol. NMR* **2003**, *25*, 243−248. (e) Ishima, R.; Baber, J.; Louis, J. M.; Torchia, D. A. *J. Biomol. NMR* **2004**, *29*, 187−198. (f) Lundström, P.; Akke, M. *ChemBioChem*, **2005**, *6*, 1685−1692.

(3) (a) McElheny, D.; Schnell, J. R.; Lansing, J. C.; Dyson, H. J.; Wright, P. E. *Proc. Natl. Acad. Sci. U.S.A.* **2005**, *102*, 5032−5037. (b) Beach, H.; Cole, R.; Gill, M. L.; Loria, J. P. *J. Am. Chem. Soc.* **2005**, *127*, 9167−9176. (c) Grey, M. J.; Wang, C.; Palmer, A. G. *J. Am. Chem. Soc.* **2003**, *125*, 14324−14335. (d) Eissenmesser, E. Z.; Millet, O.; Labeikovsky, W.; Korzhnev, D. M.; Wolf-Watz, M.; Bosco, D. A.; Skalicky, J. J.; Kay, L. E.; Kern, D. *Nature* **2005**, *438*, 117−121.

(4) Skrynnikov, N. R.; Dahlquist, F. W.; Kay, L. E. *J. Am. Chem. Soc.* **2002**, *124*, 12352−12360.

(5) (a) Trott, O.; Palmer, A. G. **2002**, *J. Magn. Res. 154*, 157−160. (b) Korzhnev, D. M.; Orekhov, V. Y.; Dahlquist, F. W.; Kay, L. E. *J. Biomol. NMR* **2003**, *26*, 39−48. (c) Korzhnev, D. M.; Orekhov, V. Y.; Kay, L. E. *J. Am. Chem. Soc.* **2005**, *127*, 713−721.

(6) van Ingen, H.; Baltussen, M. A. H.; Aelen, J. M. A.; Vuister, G. W. *J. Mol. Biol.* **2006**, in press.

(7) Levitt, M. H. *J. Magn. Reson.* **1997**, *126*, 164−182.

JA0568749

Supplementary material

CEESY: Characterizing the conformation of unobservable protein states

Hugo van Ingen, Geerten W. Vuister, Sybren Wijmenga and Marco Tessari*

Department of Physical Chemistry. Radboud University Nijmegen, Toernooiveld 1, 6525 ED, Nijmegen, The Netherlands.

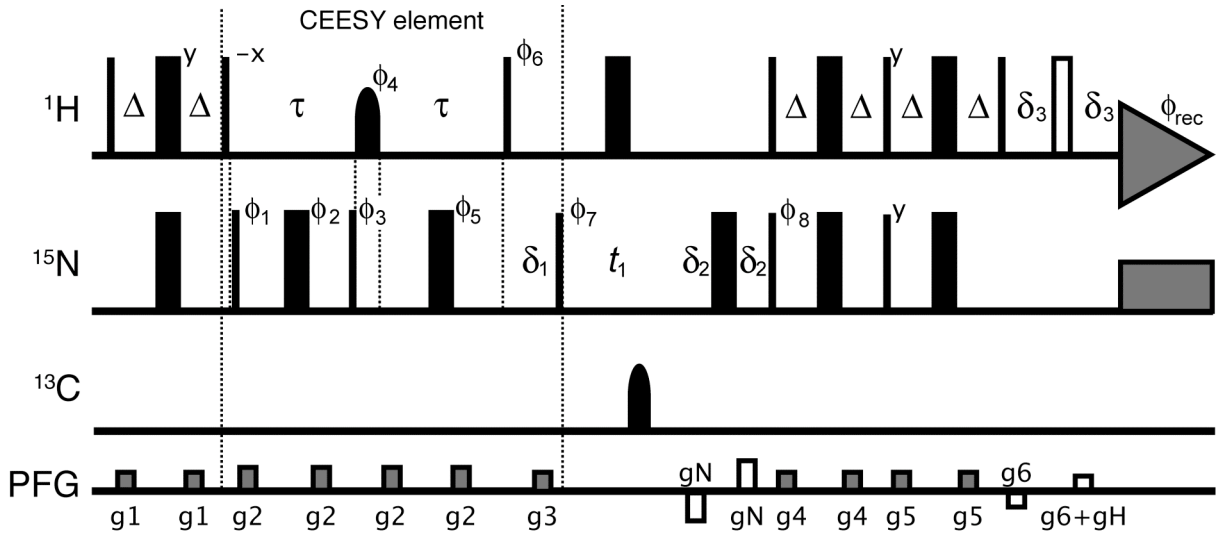

Figure S1. Pulse sequence diagram of the ^1H_N-CEESY experiment to determine sign of $\Delta\omega_{HN}$. Unless indicated otherwise, all narrow and wide closed bars represent 90° and 180° pulses along the *x*-axis, respectively. Rectangular ^{1}H (^{15}N) pulses have rf-field strengths (γB_1) of 32.4 kHz (6.1 kHz). All ^{1}H pulses during the INEPT and the CEESY block are centered on the amide region (8.53 ppm), during the *z*-filter the carrier offset is moved to 4.82 ppm. ^{15}N pulses are centered at 120.0 ppm. The shaped pulse ϕ_4 is a REBURP-shaped refocusing pulse of 2.03 ms with a peak rf-field strength of 3.0 kHz. The open bar represents the 3-9-19 implementation of the WATERGATE water suppression technique. The 180^o carbon pulse represents a sech-shaped pulse centered at 116 ppm of duration 500 μs and a peak rf-field strength of 4.1 kHz. ^{15}N WALTZ-16 decoupling during acquisition employs a 1 kHz field. Delay Δ was set to $1/4J_{NH}$ (2.65 ms), CEESY delay τ was set to 4, 8 and 12 ms, δ_1 was set to $1/2J_{NH}$ (5.3 ms), δ_2 and δ_3 to 1

ms. Recycle delay was 1.1 sec. Phase cycle (Varian Inova nomenclature): ϕ_1={*x*,-*x*}4; ϕ_2={*x*,*y*}8; ϕ_3={*x*,-*x*}16; ϕ_4={*x*,*y*}; ϕ_5={*x*,-*x*}64; ϕ_6={*y*,-*y*}2; ϕ_7={*x*,-*x*}32; ϕ_8=-*x* ϕ_{rec}={*x*,-*x*,-*x*,*x*, -*x*,*x*,*x*,-*x*, -*x*,*x*,*x*,-*x*, *x*,-*x*,-*x*,*x*, -*x*,*x*,*x*,-*x*, *x*,-*x*,-*x*,*x*, *x*,-*x*,-*x*,*x*, -*x*,*x*,*x*,-*x*, -*x*,*x*,*x*,-*x*, *x*,-*x*,-*x*,*x*, *x*,-*x*,-*x*,*x*, -*x*,*x*,*x*,-*x*, *x*,-*x*,-*x*,*x*, -*x*,*x*,*x*,-*x*, -*x*,*x*,*x*,-*x*, *x*,-*x*,-*x*,*x*}. All ^{1}H pulses executed with phase *y* or –*y* should be inverted to obtain the physically correct nutation axis[1c]. P- and N-type FIDs are recorded by adding 180° to phase ϕ_8 and inverting gradient gN. Axial peaks are shifted to edges of the spectrum by adding 180° to ϕ_7 and ϕ_{rec} every other increment. The orthogonal component of the echo formed at the end of the CEESY element is selected by adding 270° to ϕ_6, with a simultaneous 90° incrementation of all proton pulses after this pulse and of the receiver to control the state of the water magnetization. Pulsed field gradients were hyperbolic sine shaped and employed along the *z*-axis. Duration of all gradients was set to 1 ms except gradient g2 that was set to 350 μs. Gradient strengths were (in % of maximum strength, 50 G/cm): g1=3; g2=20; g3=7; g4=6; g5=9; g6=-24; gN=60; gH=12.135. Number of transients per FID was 192 for the main component and 768 for the orthogonal component (total acquisition times roughly 12/49 hours for main/orthogonal component per τ value). The spectral width of the indirect dimension was set 1200 Hz and 92 complex points were recorded. Final data size after zerofilling was 4Kx4K points. Data was recorded at 500 MHz proton frequency and 298 K with a room temperature probe-head.

To ensure accurate results, a 'zero-test' was performed by setting τ to a small value (1.6 ms) such that no significant echo rotation will occur (recorded with 512 transients per FID).

The CEESY element here is composed of MQ-evolution followed by SQ-evolution. Proper setting of phase ϕ_6 was verified experimentally[1]. In short, an unbalance was created in the echo by increasing the MQ-period with 230 μs. The echo rotation is then caused by the timing

unbalance (further ensured by using a short τ-value): $|\Omega\tau_{MQ}| > |\Omega\tau_{SQ}|$. Phase ϕ_6 was set such that the sign of the orthogonal and main component are opposite for signals with a positive offset frequency (i.e. when the main component is phased positive, the sign of the orthogonal component corresponds with $\Omega\tau_{SQ} - \Omega\tau_{MQ} < 0$).

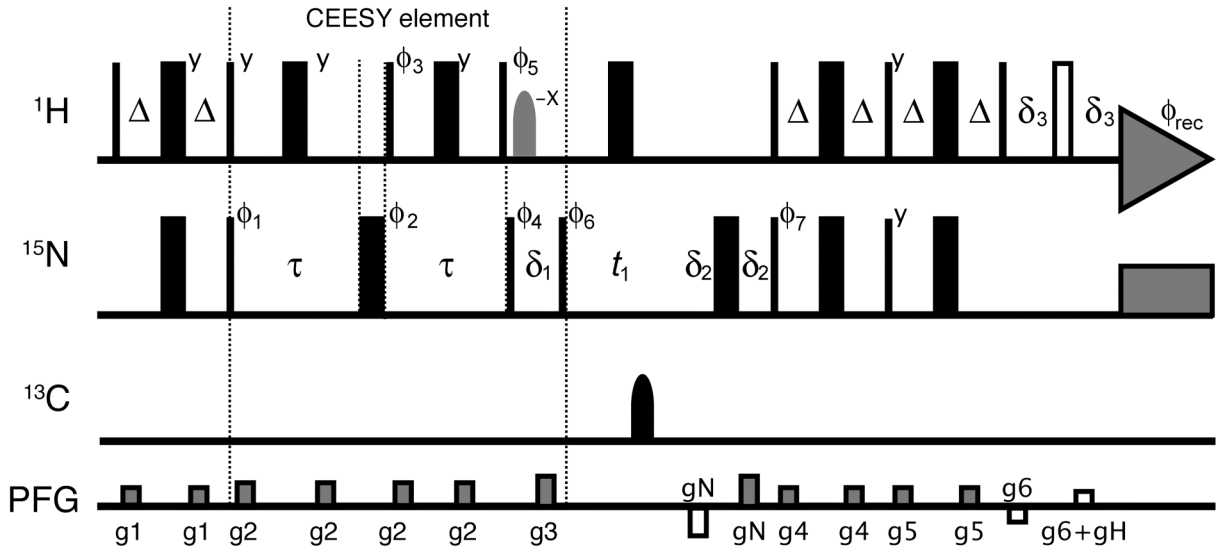

Figure S2. Pulse sequence diagram of the ^{15}N-CEESY experiment to determine sign of $\Delta\omega_N$. Unless indicated otherwise, all narrow and wide closed bars represent 90° and 180° pulses along the *x*-axis, respectively. Rectangular ^{1}H (^{15}N) pulses have rf-field strengths (γB_1) of 32.4 kHz (6.1 kHz) and are centered at 4.82 ppm (120.0 ppm). The proton shaped pulse after ϕ_5 is a sinc-shaped water-flipback pulse of 1.76 ms. The open 180° proton pulse represents the 3-9-19 implementation of the WATERGATE water suppression technique. The 180^o carbon pulse is a sech-shaped pulse centered at 116 ppm of duration 500 μs and a peak field strength of 4.1 kHz. ^{15}N WALTZ-16 decoupling during acquisition employs a 1 kHz field. Delay Δ was set to $1/4J_{NH}$ (2.5 ms), CEESY delay τ was set to 6.5, 13 and 19.5 ms, δ_1 was set to 3.5 ms, δ_2 and δ_3 to 1 ms. Recycle delay was 1 sec. Phase cycle (Varian Inova nomenclature): ϕ_1={*x*,-*x*}8; ϕ_2={*x*,*y*,-*y*,-*x*}2; ϕ_3={*y*,-*y*}16; ϕ_4={*x*,-*x*}; ϕ_5={*y*,-*y*}32; ϕ_6=*x*; ϕ_7=-*x*; ϕ_{rec}={*x*,-*x*,-*x*,*x*, -*x*,*x*,*x*,-*x*, -*x*,*x*,*x*,-*x*, *x*,-*x*,-*x*,*x*, -*x*,*x*,*x*,-*x*, *x*,-*x*,-*x*,*x*, *x*,-*x*,-*x*,*x*, -*x*,*x*,*x*,-*x*, -*x*,*x*,*x*,-*x*, *x*,-*x*,-*x*,*x*, *x*,-*x*,-*x*,*x*, -*x*,*x*,*x*,-*x*, *x*,-*x*,-*x*,*x*, -*x*,*x*,*x*,-*x*, -*x*,*x*,*x*,-*x*, *x*,-*x*,-*x*,*x*}. All ^{1}H pulses executed with phase *y* or –*y* should be inverted to obtain the physically correct nutation axis[1c]. P- and N-type FIDs are recorded by adding 180° to phase ϕ_7

and inverting gradient gN. Axial peaks are shifted to edges of the spectrum by adding 180° to ϕ_6 and ϕ_{rec} every other increment. The orthogonal component of the echo formed at the end of the CEESY element is selected by adding 270° to ϕ_4. Pulsed field gradients were hyperbolic sine shaped and employed along the *z*-axis. Duration of all gradients was set to 1 ms except gradients g2 that was set to 300 μs. Gradient strengths were (in % of maximum strength, 50 G/cm): g1=3; g2=25; g3=30; g4=6; g5=9; g6=-24; gN = 60; gH=12.161. Number of transients per FID was 80-80-320 for the main component and 640-640-1280 for the orthogonal component for τ values 6.5-13-19.5 ms (total acquisition times 4.5/41-4.5/41-18/82 hours for main/orthogonal component). The spectral width of the indirect dimension was set 1200 Hz and 100 complex points were recorded. Final data size after zerofilling was 4Kx4K points. Data was recorded at 500 MHz proton frequency and 298 K.

To ensure accurate results, a 'zero-test' was run by setting τ to a small value (1 ms) such that no significant echo rotation will occur (recorded with 384 transients per FID).

The CEESY element here is composed of SQ-evolution followed by MQ-evolution. Proper setting of phase ϕ_6 was verified experimentally[1]. In short, an unbalance was created in the echo by increasing the SQ-period with 200 μs. The echo rotation is then caused by the timing unbalance (further ensured by using a short τ-value): $|\Omega\tau_{SQ}| > |\Omega\tau_{MQ}|$. Phase ϕ_6 was set such that the sign of the orthogonal and main component are identical for signals with a positive offset frequency (i.e. when the main component is phased positive, the sign of the orthogonal component corresponds with $\Omega\tau_{SQ} - \Omega\tau_{MQ} > 0$).

Table S1. Results of the sign of $\Delta\omega_{HN}$ and $\Delta\omega_N$ using the CEESY method and comparison with the H(S/M)QC approach.

resnr.[a]	^1H_N or ^{15}N data	chemical shift (ppm)	sign[b]	SNR orthogonal component[c]	rotation echo (deg)[d]	error rotation (deg)[d]	SQ-MQ (Hz) H(S/M)QC[e]	error SQ-MQ (Hz) H(S/M)QC[e]	Δω dispersion analysis (ppm)[f]	random coil - observable (ppm)[g]
5	HN	8.27	< th.	14.8	0.882	0.057				
	N	122.93	-	-13.5	-1.025	-0.074	-0.14	0.04	1.63	-3.63
6	HN	8.51	< th.	11.6	0.670	0.057				
	N	122.13	< th.	-3.5	-0.275	-0.080	0.17	0.03	1.99	
9	HN	8.66	< th.	2.8	0.762	0.269				
	N	120.01	-	-9.4	-2.628	-0.281	-0.30	0.13		-1.01
10	HN	8.36	< th.	3.7	0.796	0.212				
	N	124.80	-	-8.8	-2.325	-0.269	-0.38	0.06	1.95	0.20
13	HN	8.10	< th.	-0.7	-0.155	-0.223				
	N	123.90	-	-4.4	-1.375	-0.309			1.98	-3.00
15	HN	8.21	< th.	0.8	0.138	0.166				
	N	117.44	< th.	-1.5	-0.338	-0.223	0.01	0.08	1.77	
17	HN	7.64	< th.	1.2	0.413	0.355				
	N	120.14	< th.	-2.8	-1.375	-0.493	-0.44	0.18	1.80	
20	HN	8.11	+	6.9	1.747	0.252				0.29
	N	123.45	-	-6.9	-2.376	-0.349	-1.25	0.17	2.63	-2.24
21	HN	7.36	< th.	-2.3	-1.071	-0.475				
	N	113.60	+	7.4	6.005	0.822	1.18	0.22	3.69	7.11
22	HN	7.25	-	-14.2	-4.141	-0.292				1.03
	N	126.05	-	-11.5	-6.153	-0.542	-1.04	0.02	5.87	-3.65
23	HN	8.68	+	10.9	2.628	0.240				-0.12
	N	113.13	+	9.2	3.234	0.355	0.89	0.22	3.15	5.97
24	HN	7.77	< th.	4.6	0.550	0.120				
	N	117.18	-	-9.2	-1.610	-0.178	-0.23	0.08	1.04	0.92
26	HN	10.31	< th.	2.9	1.409	0.487				
	N	121.59	-	-11.6	-8.093	-0.717	-1.36	0.27	2.73	-1.39
27	HN	8.17	+	4.1	1.426	0.349				0.00
	N	123.23	-	-8.6	-4.352	-0.509	-0.86	0.21	2.61	-2.83
29	HN	8.42	< th.	4.6	0.842	0.183				
	N	117.32	+	5.0	1.255	0.252	0.36	0.03	1.29	3.88
31	HN	8.26	+	8.7	1.879	0.218				0.05
	N	123.39	-	-6.5	-2.022	-0.309	-0.03	0.06	1.77	-2.69
34	HN	7.99	+	6.0	1.358	0.223				0.18
	N	122.26	-	-5.4	-1.713	-0.321	-0.01	0.22	1.48	-1.86
35	HN	7.81	< th.	0.7	0.281	0.418				
	N	119.34	+	3.9	2.159	0.561				3.06
36	HN	8.64	< th.	1.1	0.831	0.756				
	N	117.65	-	-3.2	-2.142	-0.676	-0.21	0.20	1.99	0.45
38	HN	8.28	< th.	-1.6	-0.487	-0.315				

resnr.[a]	$^{1}H_N$ or ^{15}N data	chemical shift (ppm)	sign[b]	SNR orthogonal component[c]	rotation echo (deg)[d]	error rotation (deg)[d]	SQ-MQ (Hz) H(S/M)QC[e]	error SQ-MQ (Hz) H(S/M)QC[e]	$\Delta\omega$ dispersion analysis (ppm)[f]	random coil - observable (ppm)[g]
	N	122.17	-	-5.2	-2.148	-0.412	-1.21	0.17	1.27	-1.27
40	HN	7.98	< th.	2.3	0.355	0.155				
	N	119.49	< th.	-2.1	-0.453	-0.218	-0.05	0.17	1.44	
41	HN	8.06	< th.	5.0	0.814	0.166				
	N	118.93	< th.	-3.8	-0.888	-0.235	-0.02	0.11	1.50	
42	HN	7.88	< th.	3.6	0.791	0.218				
	N	117.72	+	5.1	1.570	0.304	0.33	0.33	2.10	2.78
43	HN	7.73	< th.	2.1	0.401	0.195				
	N	120.06	< th.	-0.5	-0.132	-0.252	0.12	0.11	1.86	
44	HN	8.23	+	3.2	1.919	0.596				
	N	119.17	< th.	-1.8	-1.237	-0.693	-1.21	0.21	2.32	
46	HN	8.42	< th.	3.3	0.796	0.241				
	N	123.92	-	-7.1	-1.844	-0.263	-0.25	0.05	1.95	-2.32
47	HN	8.65	< th.	1.7	1.873	1.083				
	N	110.58	-	-5.0	-6.045	-1.233	-0.85	0.69		-3.08
51	HN	8.33	+	3.8	1.381	0.361				
	N	124.17	-	-8.2	-4.021	-0.492	-0.56	0.34	3.69	-2.97
52	HN	7.81	< th.	0.6	0.229	0.390				
	N	109.84	-	-4.4	-1.919	-0.430	0.19	0.31		-2.34
53	HN	8.53	+	3.2	1.392	0.435				
	N	121.10	-	-12.5	-6.124	-0.497	-0.64	0.17	1.80	-0.80
54	HN	8.95	+	10.3	3.028	0.298				-0.52
	N	120.48	-	-7.5	-3.622	-0.486	-1.06	0.32	4.12	-4.98
55	HN	9.03	< th.	5.6	0.940	0.172				
	N	121.33	< th.	2.9	0.607	0.212	0.26	0.01	1.03	
56	HN	8.70	< th.	5.7	0.917	0.160				
	N	118.48	< th.	-4.0	-0.882	-0.223	-0.07	0.05	1.33	
59	HN	8.27	+	7.6	1.243	0.166				0.04
	N	119.42	-	-6.5	-1.472	-0.229	0.06	0.14	1.74	1.28
61	HN	7.99	< th.	4.2	0.653	0.155				
	N	120.56	< th.	2.4	0.516	0.218	0.16	0.08	1.44	
63	HN	8.47	< th.	2.5	0.321	0.126				
	N	122.17	-	-6.6	-1.163	-0.178	-0.22	0.00		1.28
64	HN	7.46	< th.	1.8	0.630	0.349				
	N	114.33	+	6.2	2.862	0.464	0.58	0.38		4.67
66	HN	8.15	< th.	2.3	0.877	0.372				
	N	114.85	< th.	-1.3	-0.693	-0.539	-0.32	0.27	1.59	
67	HN	7.02	< th.	-0.4	-0.103	-0.252				
	N	120.83	-	-3.8	-1.180	-0.315	0.02	0.30	1.15	0.37
68	HN	9.35	+	4.2	4.853	1.172				-0.94
	N	115.26	-	-6.7	-10.869	-1.693	-2.13	1.21	4.46	-7.76
69	HN	8.50	< th.	2.9	0.401	0.138				
	N	120.50	-	-14.4	-2.960	-0.206	-0.50	0.01	1.04	0.00
71	HN	8.98	< th.	7.8	0.842	0.109				

resnr.[a]	^1H_N or ^{15}N data	chemical shift (ppm)	sign[b]	SNR orthogonal component[c]	rotation echo (deg)[d]	error rotation (deg)[d]	SQ-MQ (Hz) H(S/M)QC[e]	error SQ-MQ (Hz) H(S/M)QC[e]	$\Delta\omega$ dispersion analysis (ppm)[f]	random coil - observable (ppm)[g]
	N	119.29	< th.	-6.5	-0.928	-0.143	-0.05	0.05	1.18	
72	HN	7.78	< th.	-1.1	-0.183	-0.172				
	N	119.60	+	5.4	1.318	0.246	0.26	0.05	2.66	2.80
73	HN	8.05	< th.	5.5	0.814	0.149				
	N	119.98	-	-7.2	-1.518	-0.212				2.42
76	HN	7.85	-	-5.8	-2.554	-0.441				0.46
	N	121.44	-	-4.9	-4.067	-0.841	-0.80	0.19	6.68	-0.74
79	HN	7.51	< th.	-0.6	-0.854	-1.490				
	N	120.40	< th.	-2.0	-6.113	-3.077	-0.51	0.62	5.51	
84	HN	7.97	-	-5.6	-1.226	-0.223				0.39
	N	116.05	< th.	2.2	0.665	0.309	0.00	0.11	3.95	
85	HN	7.58	-	-4.5	-5.148	-1.171				0.81
	N	119.70	+	10.8	19.565	2.119	3.22	0.90	6.23	1.50
87	HN	8.04	< th.	-1.3	-0.395	-0.315				
	N	121.98	< th.	-3.0	-1.232	-0.412	0.16	0.23	2.32	
89	HN	7.97	< th.	-2.2	-0.842	-0.384				
	N	112.74	< th.	-2.3	-0.607	-0.269	0.17	0.09	2.69	

[a] only those residues are shown for which either the sign of $\Delta\omega_{HN}$ or $\Delta\omega_N$ was determined or significant ^{15}N-R_2 dispersion was observed.

[b] sign based on the CEESY-experiment. Criteria: signal-to-noise > 3 and echo rotation > 1^o. Residues for which no sign could be determined are indicated by "< th."

[c] Signal-to-Noise Ratio for the orthogonal component observed in the spectra with the longest echo delay (12 ms for ^1H_N and 19.5 ms for ^{15}N).

[d] echo rotation (α) for τ = 12 ms (^1H_N) or 19.5 ms (^{15}N) was calculated using the relation: $\alpha = \arctan(I_{ortho}/I_{main})$, in which I_{ortho} and I_{main} are the intensities in the orthogonal and main component, both rescaled to 1 scan to compensate for the difference in acquisition time. Errors are based on the noise-level.

[e] difference in peak position along the ^{15}N-dimension between HSQC and HQMC spectra. Average value and standard deviation of three measurements. HSQC and HMQC spectra were recorded interleaved at 500 MHz proton frequency; spectral width of the indirect dimension was set to 1200 Hz; 92 complex points; 64 transient per FID.

[f] magnitude of the ^{15}N chemical shift difference between excited and ground state as determined by a global fit of CPMG ^{15}N R_2-relaxation dispersion data. Dispersion curves were recorded at 298K and 500, 600 and 800 MHz proton frequency. Curves were fit to the Carver-Richards-Jen[2] all time scale approximation describing the apparent R_2 as function of the pulse spacing in CPMG experiments.

[g] chemical shift difference between the random coil shift and the ground state $^{1}H_N$ or ^{15}N shift. Random coil shifts based on the Wright & Dyson values deposited in the BMRB database[3].

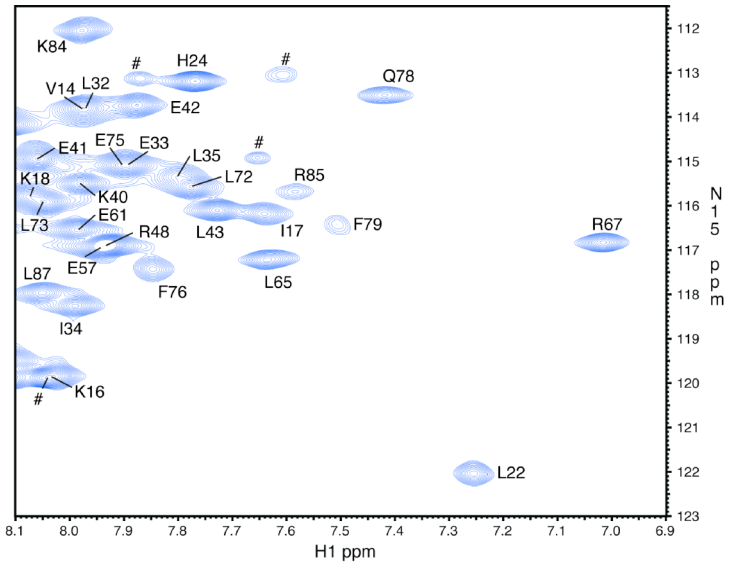
K84
#
H24
#
Q78
V14
L32
E42
E41
E75
E33
L35
#
K18
L72
R85
K40
L73
E61
L43
I17
F79
R67
R48
E57
L87
F76
L65
I34
#
K16
L22
112
113
114
115
116
117
118
119
120
121
122
123
N 1 5 p p m
8.1
8.0
7.9
7.8
7.7
7.6
7.5
7.4
7.3
7.2
7.1
7.0
6.9
H1 ppm

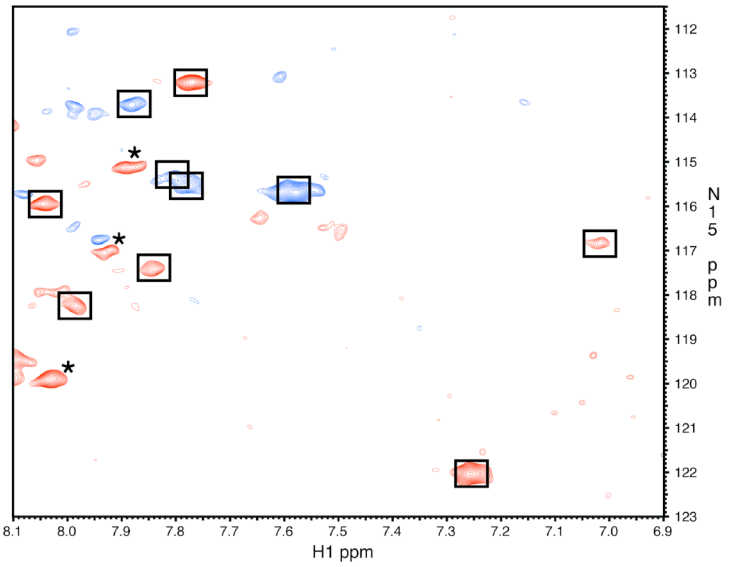
*
*
*
112
113
114
115
116
117
118
119
120
121
122
123
N 1 5 p p m
8.1
8.0
7.9
7.8
7.7
7.6
7.5
7.4
7.3
7.2
7.1
7.0
6.9
H1 ppm

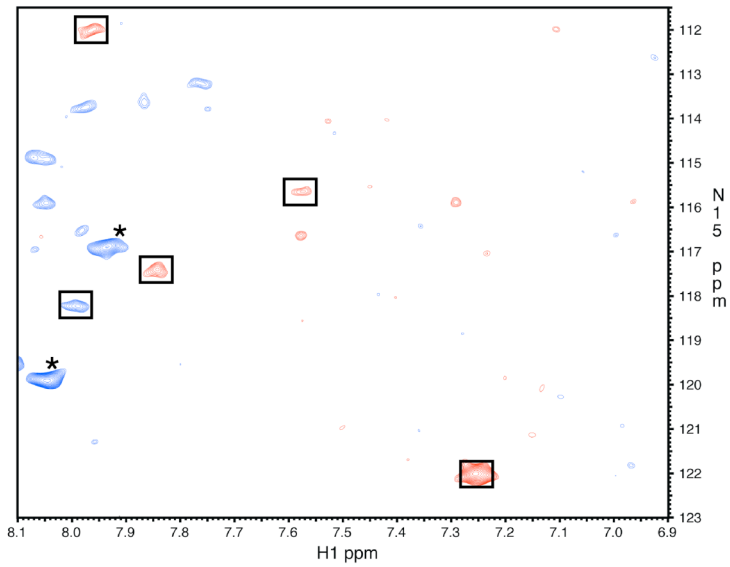
*
*
112
113
114
115
116
117
118
119
120
121
122
123
N 1 5 p p m
8.1
8.0
7.9
7.8
7.7
7.6
7.5
7.4
7.3
7.2
7.1
7.0
6.9
H1 ppm

Figure S3. Sections of the 2D spectra of a reference $^{1}H,^{15}N$-HSQC spectrum (top panel), the orthogonal component spectrum of the ^{15}N-CEESY experiment (CEESY delay τ is 19.5 ms; middle panel) and the orthogonal component spectrum of the ^{1}H-CEESY experiment (CEESY delay τ is 12 ms; bottom panel). Positive and negative peaks are coloured blue and red, respectively. The othogonal component spectra are contoured at the noise level. The assignment of the resonances is shown in the top panel. Peaks labeled with a hash (#) result from fragments due to protein degradation. Peaks in the orthogonal component spectra that fulfill the criteria described in the main text (SNR > 3 and $\arctan(I_{ortho}/I_{main}) > 1^{o}$), are enclosed in boxes and were used to classify the sign of the frequency difference between the ground and excited state (see also Table S1). Peaks labeled with a star (*) are not considered due to overlap.

Supplementary references:

1. (a) Levitt, M.H. *J. Magn. Reson.* **1997**, *126*, 164-182. (b) Levitt, M.H.; Johannessen, O.G. *J. Magn. Reson.* **2000**, *142*, 190-194. (c) Roehrl, M.H.; Heffron, G.J.; Wagner, G. *J. Magn. Reson.* **2005**, *174*, 325-330.

2. (a) Carver, J.P.; Richards, R.E. **1977**, *J. Magn. Res.*, *6*, 89-105. (b) Jen, J. **1978**, *J. Magn. Res.*, *30*, 111-128.

3. Schwarzinger, S.; Kroon, G. J. A.; Foss, T.R.; Wright, P. E.; Dyson, H. J. **2000**, *J. Biomol. NMR*, *18*, 43-48.